J Mater Sci (2009) 44:5509–5514
DOI 10.1007/s10853-009-3769-0

Thermal properties and microstructure of bulk nanocrystalline Gd material

Hong Zeng · Chunjiang Kuang · Jiuxing Zhang · Ming Yue

Received: 16 April 2009 / Accepted: 21 July 2009 / Published online: 4 August 2009

Abstract Bulk nanocrystalline gadolinium (Gd) material has been consolidated from Gd nanoparticles using spark plasma sintering (SPS). High density (>99.5%) bulk nanocrystalline material was achieved after sintering at a temperature of 280 °C with a pressure of 500 MPa. Microstructure analysis shows that the consolidated bulk material exhibits a single phase with hexagonal close packed structure and a fine grain microstructure with a mean grain size of about 15 nm. The structural transformation from hexagonal condensed packed to face centered cubic was not observed, and the second-order magnetic transition remained in the nanocrystalline Gd sample. The Curie temperature of the nanocrystalline Gd decreased by more than 10.7 K below that of the coarse-grained. The activation energies for the coarse-grained and the as-consolidated Gd materials are 2.7702 and 1.0130 eV, respectively.

Introduction

In recent years, the nanoscale materials received considerable attention because they showed novel properties that are markedly different from those of the traditional materials, due to the small-size effects and quantum-size effects. The metal gadolinium (Gd), the only simple ferromagnet among the rare earth elements at room temperature, has drawn tremendous attention and was broadly investigated for the past decades [1–3]. Consequently, considerable investigation has been devoted to the synthesis of many kinds of nanostructural Gd materials including clusters, thin films, particles, and their green compacts [4–9]. However, until now, the research on full dense bulk nanocrystalline Gd is relatively rare. This is due to the difficulties encountered in the synthesis of pure bulk nanocrystalline Gd materials, resulting from its high reactivity and low resistance to oxidation. Besides, in the synthesis process by the common consolidation methods, the energy (at high temperatures) required to densify nano powders may cause the grains to grow up to micrometer size.

In our recent research, a novel technique was developed to prepare full dense bulk size-controllable nanocrystalline pure rare earth metals [10], which enabled us to study the influence of nanostructure on the thermal properties of Gd.

Experimental

The Gd nanoparticles were prepared by the inert-gas condensation technique [6]. The pure bulk Gd metal (99.9%) to be evaporated was laid on the water-cooled copper anode; the vacuum chamber was pumped to 10^{-4} Pa and then was backfilled with helium gas to the desired pressure. The distance between tungsten cathode and a copper anode can be adjusted from outside the vacuum chamber, so that the arc plasma can be easily initiated and controlled. During the operation, the pure bulk Gd metal was heated, melted, and evaporated into atom smoke of the metal by the high temperature of the arc plasma. The Gd nanoparticles were

H. Zeng (✉) · C. Kuang
Advance Technology & Materials Co., Ltd.,
China Iron & steel Research Institute Group, Beijing 100081,
People's Republic of China
e-mail: zenghong78@live.cn

J. Zhang · M. Yue
The Key Laboratory of Advanced Functional Materials, Ministry of Education, Beijing University of Technology, Beijing 100022,
People's Republic of China

formed by collision between the metal atoms, after the metal atoms collided with helium gas atoms and lost their energy.

The spark plasma sintering (SPS) is a novel technique to make powders into bulk nanocrystalline materials [11]. The nano-Gd powders were sintered by using SPS (SPS-5.40-IV/ET, Sumitomo Coal Mining Co., Ltd., Japan). The prepared Gd nanoparticles were pressed in hard WC die (20-mm diameter) under argon atmosphere with oxygen concentration below 1 ppm, which efficiently inhibits oxidation of the nanoparticles. The sintering was carried out in vacuum, at a temperature of 280 °C, under the pressure of 500 MPa and without heat preservation time. After sintering, the consolidated bulk material was cooled down to room temperature.

The crystal structure and the phase purity and composition of the nanoparticles, the consolidated bulk material, and the raw sample were examined by X-ray diffraction (XRD) with Cu Kα radiation. The crystallite size was calculated using the relation: $d = k\lambda/B\cos\theta$, where d is diameter, k is a constant (= 0.9), B is the half-maximum line width, and λ is the wave length of the X-rays. The morphology of the nanoparticles and the microstructure of the consolidated bulk pure Gd metal were observed with PHILIPS TECNAIF30 (operated at 300 kV) transmission electron microscopes (TEM) and select area electron diffraction (SAED).

The density of the consolidated sample was determined by the Archimedes method to be approximately over 99.5% of that of bulk Gd. This density of the bulk nanocrystalline material is considered to be very high.

Thermal analysis was carried out using differential scanning calorimeter (DSC).

Results and discussion

The lattice structure and the phase purity of the nanoparticles of the rare earth Gd metal, which was prepared by the inert-gas condensation method, are very difficult to determine by XRD due to the oxidation and burning of the nanoparticles. However, it can be easily estimated from the XRD result of the nanocrystalline bulk Gd materials, which is shown in Fig. 3. It shows the nanoparticles are mainly composed of the Gd phase.

The TEM images of the Gd nanoparticles prepared by the inert-gas condensation are shown in Fig. 1. The Gd nanoparticles have nearly hexagonal shape and the size distribution of the nanoparticles is very narrow, ranging from 10 to 70 nm with a mean particle size of 40 nm. It was also found that the as-prepared Gd nanoparticles have integral surface and no defects and these nanoparticles are connected together.

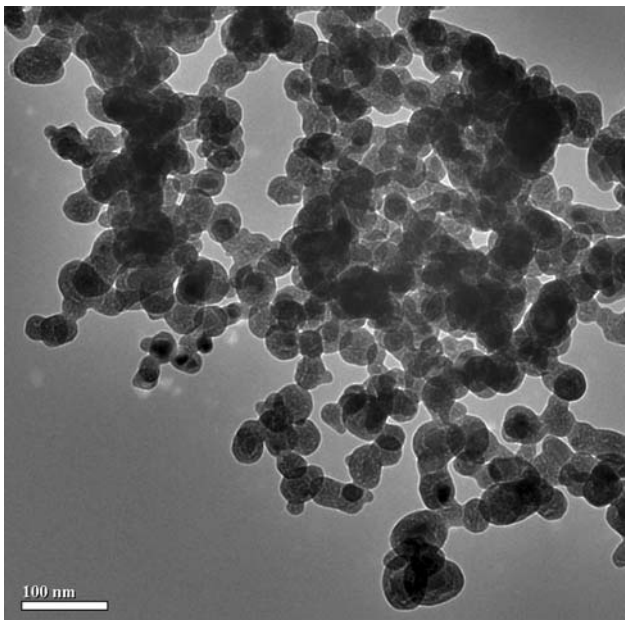

Fig. 1 TEM micrograph of nano-particles Gd prepared by the inert-gas condensation

In order to get more information on the Gd nanoparticles, high-resolution transmission electron microscopy (HRTEM) with SAED analysis was used. Figure 2 is the atom crystal image. It is revealed that the space between the atom surfaces in a single nanoparticle is 2.880 Å, which corresponds with the (002) crystal field of the Gd hexagonal close packed (HCP) crystal structure. In the meantime, it also provides the proof that the nanoparticles

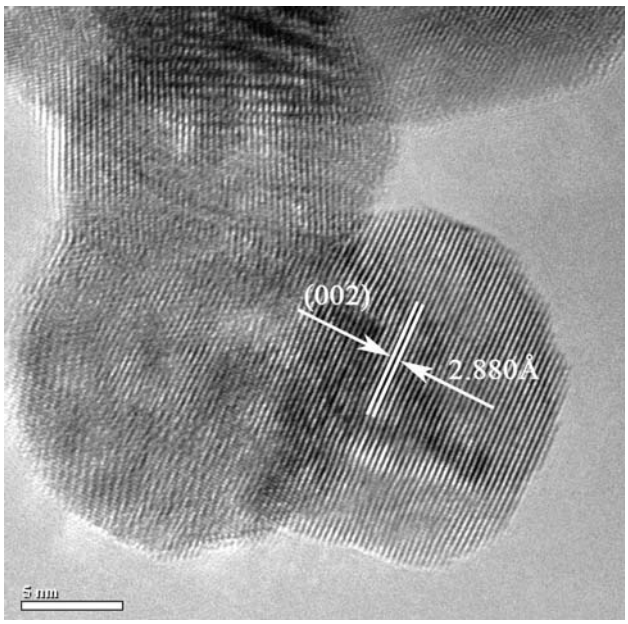

Fig. 2 HETEM micrograph of nano-particles Gd prepared by the inert-gas condensation

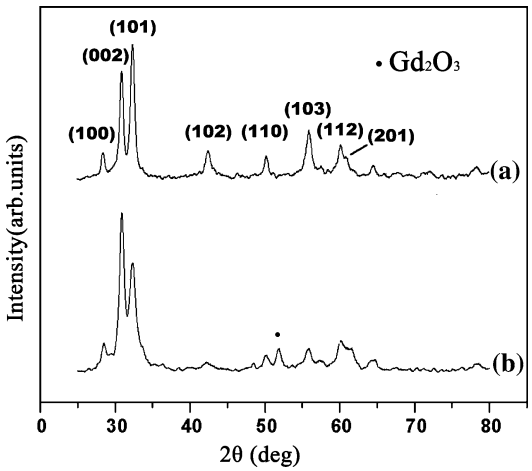

Fig. 3 XRD patterns of the rare earth metal Gd: (a) raw material and (b) the as-consolidated

prepared by the inert-gas condensation are single-crystal nanoparticles.

Figure 3 shows the XRD patterns for a coarse-grained polycrystalline Gd raw material and the as-consolidated sample. The Bragg peaks of the bulk Gd samples, arising only from the equilibrium HCP phase and not from metastable face centered cubic (FCC) Gd, are composed of a single pure HCP phase of Gd. It can also be seen that the diffraction peaks of the as-consolidated sample are broader than those of the coarse-grained polycrystalline Gd raw material due to the small sizes of the crystal grains in the samples, indicating that the crystal size of the coarse-grained Gd is coarser than that of the as-consolidated. The average crystal sizes of the consolidated bulk nanocrystalline Gd sample, calculated using Scherer's formula, are about 14.4 nm, which is in agreement with the later TEM observations (Fig. 5). In addition, an extra diffraction peak around 2θ of 52°, which does not belong to the Gd metal, appeared in the consolidated Gd sample. Further indexing indicates that it is a kind of Gd_2O_3 impurity with a monoclinic structure.

Figure 4 shows typical TEM images and the SAED patterns of the coarse-grained polycrystalline Gd raw material. It is revealed from Fig. 4a that the mean grain size of the coarse-grained Gd sample is over 1000 nm. From the corresponding SAED (Fig. 4b), the existence of HCP Gd can be confirmed by the characteristic diffraction spots from single-crystal, the indexing of the SAED pattern indicating the characteristic lattice planes (002), (110),(112) of HCP Gd. The results are consistent with the XRD results (Fig. 3).

Figure 5 shows typical TEM images and the SAED patterns of the consolidated bulk nanocrystalline Gd material. The TEM image of the consolidated bulk nanocrystalline Gd is shown in Fig. 5a. It is revealed from the TEM micrograph observation that the grain sizes in the as-consolidated sample narrow range from 9 to 15 nm with a mean size of about 13 nm. The homogeneous microstructures may be caused by the SPS unique sintering mechanism. Figure 5b shows the corresponding SAED of the nanocrystalline Gd, which is consistent with the crystallinity of the sample and reveals seven diffraction rings in accordance with the (100), (002), (101), (102), (110), (112), and (210) crystal planes of *hcp* phase Gd. So, the corresponding indexing of the SAED pattern indicates that the nanosized crystal grains have the same equilibrium HCP crystal structure as common coarse-grained Gd.

In order to observe the interface of the nanocrystalline Gd and get more detailed information about nanocrystalline Gd, the amplification of bulk Gd material is used (Fig. 6). As can be seen from Fig. 6, the actual grain sizes attain to 15 nm, which is in contrast with the previous 13 nm (Fig. 5). Meanwhile, the nanograins have the different orientations in the HRTEM micrograph. The space between the atom surfaces in a single-nanocrystal is 3.1435 Å, which is coincident with the (100) crystal field

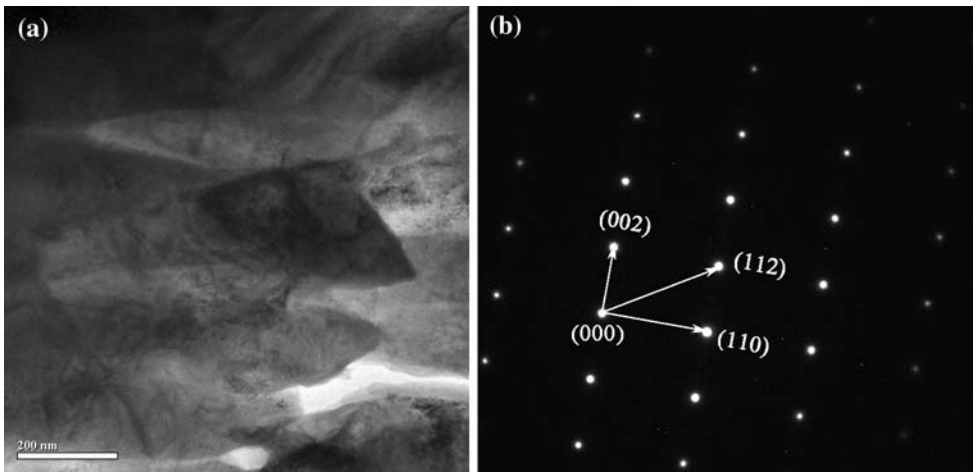

Fig. 4 **a** TEM micrograph of the polycrystalline Gd and **b** the corresponding SAED patterns

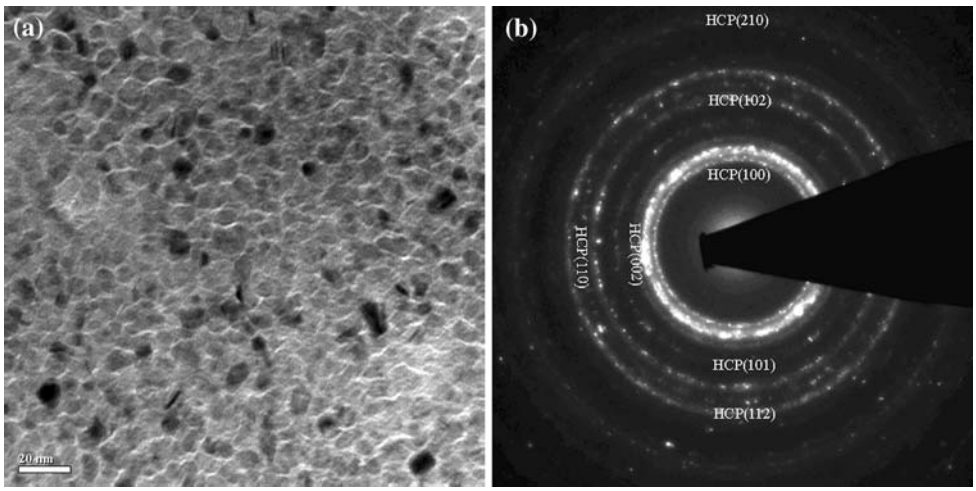

Fig. 5 **a** TEM micrograph of the as-consolidated Gd and **b** the corresponding SAED patterns

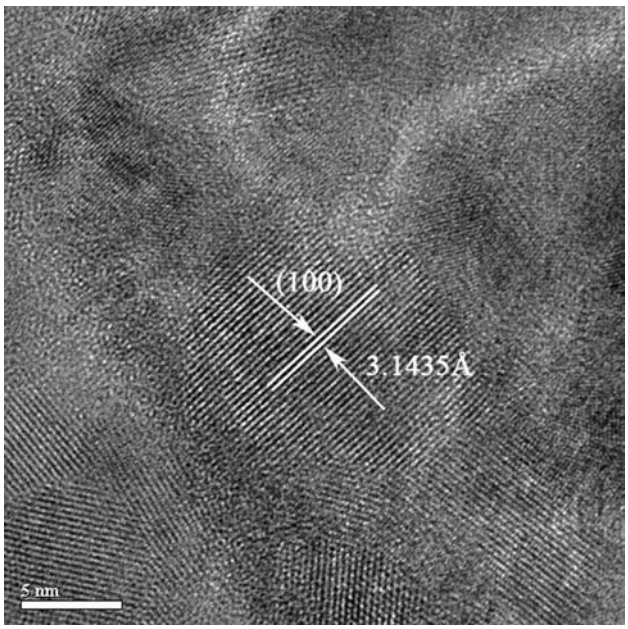

Fig. 6 HETEM micrograph of the consolidated bulk nanocrystalline Gd

of Gd HCP crystal structure. It is also found that the maximum width of grain boundary with amorphous state is about 2 nm. The formability of the special microstructure in the bulk nanocrystalline Gd material is attributed to SPS's unique sintering mechanism and the character of the raw nano-particles. By controlling SPS conditions or the annealing process, dense homogeneous microstructures with different grain sizes as low as 20–100 nm can also be obtained.

In the research, no evidence was seen for the FCC Gd phase in either the XRD or TEM data. This indicates that the nanosized Gd crystal grains still possess HCP structure. Namely, the variations of grain size in present conditions do not cause their structural transformations from HCP to FCC in the bulk Gd materials, which can take place in the Gd nanoparticles when the crystal grain size reaches certain scale [6–8]. The size-induced transformations in nanoparticles can be explained due to the modified surface structure, large concentration defects present in the nanophase, or a change in the Gibbs free energy due to surface energy term [12, 13]. As mentioned above, the mean grain sizes in the as-consolidated nanocrystalline Gd sample is about 15 nm. So, the reduction size could not attain the critical point, at which the structure transformations from HCP to FCC in the bulk Gd materials take place. Meanwhile, the concentration defects, once largely presented in the nanoparticles, may be less in the bulk nanocrystalline Gd materials. Moreover, the HCP Gd is an equilibrium phase, but the FCC Gd is a metastable phase [14]. Compared with the Gd nanoparticles, the bulk nanocrystalline Gd material behaves steady state. The phenomena, however, are not observed in our bulk nanocrystalline Gd materials which maybe due to the larger crystal grain size and the different nanostructure states, especially the bulk nanocrystalline in our study.

Figure 7 shows the calorimetric traces of the as-consolidated and coarse-grained bulk Gd samples at the heating rate of 20 K/min. To our knowledge, the paramagnetic–ferromagnetic phase transition in polycrystalline coarse-grained Gd is the second-order magnetic transition. However, the trace of the bulk nanocrystalline Gd materials is like "λ" shape with the obvious characteristic of second-order transition, indicating that the second-order paramagnetic–ferromagnetic phase transitions take place in the bulk nanocrystalline sample. In other words, nanostructures do not change the magnetic transition and still preserve the second-order magnetic transition in the bulk nanocrystalline Gd material. At the same time, all traces exhibit an obvious endothermic peak due to the second-order ferromagnetic → paramagnetic phase transition, which can be identified with the Curie temperature T_C [5, 15, 16].

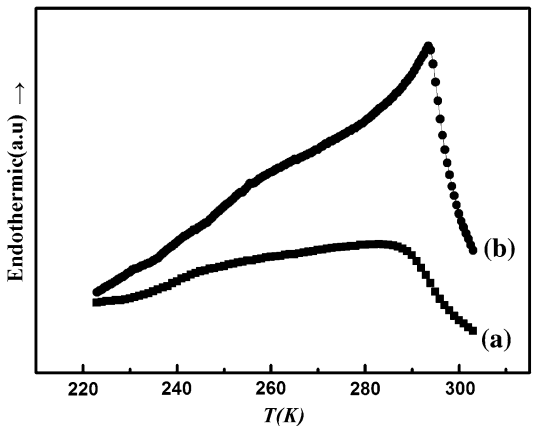

Fig. 7 The calorimetric traces of the bulk Gd samples: **a** the as-consolidated and **b** the raw material

As illustrated in Fig. 7b, the sharp peak of coarse-grained Gd located at 293.6 K is very close to the literature value for T_C in Gd (294 K [3]). In contrast, the corresponding curve for the nanocrystalline Gd material with 15 nm manifests a broader, more rounded peak, and the temperature of the maximum heat flow is 282.9 K shown in Fig. 7a. So, the T_C peak temperatures are strongly dependent on the crystallite size of the bulk Gd materials and the temperatures of the Gd turn out to be reduced to 10.7 K. The broadening of T_C peak in the as-consolidated sample comparison with the coarse-grained bulk Gd sample, can be at least partially, attributed to the structural disorder due to the significantly increased total grain boundary area in the bulk nanocrystalline material. A similar phenomenon, related to the finite size effect, has been found in previous studies for Gd nanoparticles and thin films [4–6], also widely observed in other nanocrystalline ferromagnetic systems [17, 18].

The kinetic analysis of the magnetic phase transition of the as-consolidated and raw samples has been performed by using Kissinger's method [19]. Figure 8 shows the DSC curves obtained from the as-consolidated and raw samples at different heating rates. The effective activation energies for the magnetic phase transition (ferromagnetic → paramagnetic) can be obtained using the following equation [19]:

$$\ln\left(T^2/\beta\right) = \ln(E_a/k_B K_0) + E_a/k_B T, \quad (1)$$

where β is the heating rate, k_B is the Boltzmann constant, K_0 is the frequency factor, and E_a is the apparent activation energy. The calculated values of E_a are 2.7702 and 1.0130 eV for the coarse-grained and the as-consolidated, respectively. The coarse-grained bulk Gd has relatively large value of E_a, indicating that the atoms of coarse-grained Gd sample need larger additional energy for the second-order transition from ferromagnetic phase state to

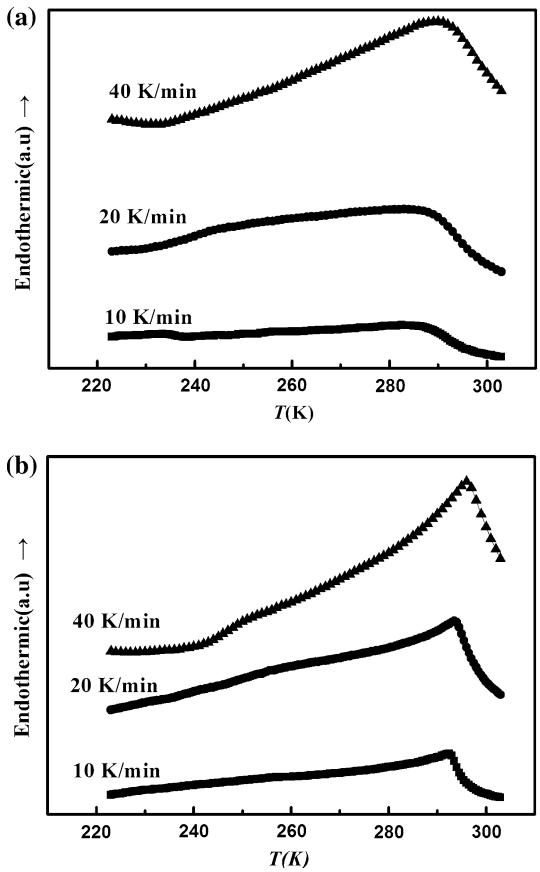

Fig. 8 DSC curves (10, 20, 40 K/min) of the rare earth metal Gd: **a** the as-consolidated and **b** the raw material

paramagnetic phase state compared to that of the bulk nanocrystalline Gd metal. The high transition temperature and large activation energy imply that the ferromagnetic phase in coarse-grained Gd sample has high thermal stability with respect to the bulk nanocrystalline Gd.

Conclusions

In summary, full dense bulk pure nanocrystalline Gd material has been synthesized through combining the inert-gas condensation with the SPS technology. The SPS Gd metal with a single HCP phase and a mean grain size of about 15 nm is obtained. The formation of the fine grain microstructure is a result of both the SPS consolidation mechanism and the intrinsic properties of the initial nanoparticles. The structural transformation from HCP to FCC does not take place in the nanocrystalline bulk Gd materials. Meanwhile, the nanostructure does not change the magnetic transition and still preserve the second-order magnetic transition. However, the Curie temperature T_C of nanocrystalline Gd is more than 10.7 K below that of coarse-grained polycrystalline Gd, and manifests a broader

shape than the coarse-grained ones. The activation energies (E_a) for the coarse-grained and the as-consolidated samples, calculated using Kissinger's method, are 2.7702 and 1.0130 eV, respectively.

References

1. Geldart DJW, Hargraves P, Fujiki NM, Dublap RA (1962) Phys Rev 132:2728
2. Nakamura O, Baba K, Ishii H, Takeda T (1988) J Appl Phys 64:3614
3. Dan'kov SY, Tishin AM, Pecharsky VK, Gschneidner KA Jr (1998) Phys Rev B 57:3478
4. O'shea MJ, Perera P (1999) J Appl Phys 85:4322
5. Aly SH (2000) J Magn Magn Mater 222:368
6. Michels D, Krill CEIII, Birringer R (2002) J Magn Magn Mater 250:203
7. Aruna I, Mehta BR, Malhotra LK et al (2004) Adv Mater 16:169
8. Aruna I, Mehta BR, Malhotra LK et al (2005) Adv Funct Mater 15:131
9. Kruk R, Ghafari M, Hahn H, Michels D, Birringer R, Krill CEIII, Kmiec R, Marszalek M (2006) Phys Rev B 73:054420
10. Song X, Zhang J, Yue M, Li E, Zeng H, Lu N, Zhou M, Zuo T (2006) Adv Mater 18:1210
11. Gao L, Li Q, Luan W (2002) J Am Ceram Soc 85:1016
12. Wickham JN, Herhold AB, Alivisatos AP (2000) Phys Rev Lett 84:923
13. Balamurugan B, Mehta BR, Shivaprasad SM (2001) Appl Phys Lett 79:3176
14. Chizov PE, Kostigov AN, Petinov VI (1982) Solid State Commun 42:323
15. Herrero-Albillos J, Casanova F, Bartolome F, Garcia LM, Labarta A, Batlle X (2005) J Magn Magn Mater 290–291:682
16. Herrero-Albillos J, Bartolome F, Garcia LM, Casanova F, Labarta A, Batlle X (2006) Phys Rev B 73:134410
17. Sato T, Iijima T, Seki M, Inagaki N (1987) J Magn Magn Mater 65:252
18. Löffler JF, Meier JP, Doudin B, Ansermet JP, Wagner W (1998) Phys Rev B 57:2915
19. Kissinger HE (1956) J Res Natl Bur Stand 57:217